Published online 3 March 2009

Nucleic Acids Research, 2009, Vol. 37, No. 8 ***2471–2482***
doi:10.1093/nar/gkp055

Natural isoflavones regulate the quadruplex–duplex competition in human telomeric DNA

Jin-li Zhang[1], Yan Fu[1], Lin Zheng[1], Wei Li[2,*], Hao Li[3], Qian Sun[2], Ying Xiao[1] and Feng Geng[1]

[1]Key Laboratory of Systems Bioengineering, [2]Key Laboratory for Green Chemical Technology, Ministry of Education, School of Chemical Engineering & Technology, Tianjin University, Tianjin 300072 and [3]Qilu Hospital of Shandong University, Jinan 250012, Shangdong Province, China

Received November 22, 2008; Revised January 18, 2009; Accepted January 19, 2009

ABSTRACT

Effects of natural isoflavones on the structural competition of human telomeric G-quadruplex d[$AG_3(T_2AG_3)_3$] and its related Watson–Crick duplex d[$AG_3(T_2AG_3)_3$-$(C_3TA_2)_3C_3T$] are investigated by using circular dichroism (CD), ESI-MS, fluorescence quenching measurement, CD stopped-flow kinetic experiment, UV spectroscopy and molecular modeling methods. It is intriguing to find out that isoflavones can stabilize the G-quadruplex structure but destabilize its corresponding Watson–Crick duplex and this discriminated interaction is intensified by molecular crowding environments. Kinetic experiments indicate that the dissociation rate of quadruplex ($k_{obs290\,nm}$) is decreased by 40.3% at the daidzin/DNA molar ratio of 1.0 in K^+, whereas in Na^+ the observed rate constant is reduced by about 12.0%. Furthermore, glycosidic daidzin significantly induces a structural transition of the polymorphic G-quadruplex into the antiparallel conformation in K^+. This is the first report on the recognition of isoflavones with conformational polymorphism of G-quadruplex, which suggests that natural isoflavone constituents potentially exhibit distinct regulation on the structural competition of quadruplex versus duplex in human telomeric DNA.

INTRODUCTION

G-quadruplex forming sequences have been found to be prevalent in all eukaryotic chromosomes, particularly enriched in telomeric regions (1,2), insulin-linked polymorphic region (3), regulatory sequences of muscle-specific genes (4) and upstream of transcription initiation sites of proto-oncogenes such as *c-myc* (5), *c-kit* (6), *bcl-2* (7), *VEGF* (8) and *RET* (9). Interconversion mechanism between the G-quadruplex and the Watson–Crick (WC) duplex structures is fundamental to understand how the gene transcription is regulated *in vivo* and how to design potent anticancer drugs in the field of medicinal chemistry (5,10–13), as well as how to construct nanomolecular machines based on supramolecular assembly of nucleic acids (14–16).

A number of studies suggested that the structural competition between the G-quadruplex and its corresponding duplex is dependent upon cationic conditions, pH, temperature, loop length of G-quadruplex and molecular crowding agent (17–21). Recently, several classes of ligands, involving telomestatin (22), a platinum supramolecular square (23), macrocyclic oligoamide (24), a nickel salen complex (25), trisubstituted isoalloxazine (11) and oxazole-based peptide macrocycles (26), were reported to stabilize the G-quadruplex with less or no increasing effects on the stability of the duplex. In additions, Dixon *et al.* (27) reported a high quadruplex-affinity compound, a pentacationic manganese(III) porphyrin combining a central aromatic core and four flexible cationic arms, which is able to discriminate between the quadruplex and the duplex DNA by four orders of magnitude and cause inhibition of telomerase at submicromolar concentration ($IC_{50} = 580$ nM). Balasubramanian *et al.* (28) investigated the influence of a hemicyanine-peptide ligand on the quadruplex unfolding with a complementary oligonucleotide and suggested that the ligand retards duplex formation significantly owing to a relatively large decrease in entropy induced by the formation of quadruplex–ligand complex. These quadruplex-stabilized ligands are considered as potential anticancer candidates for their ability to inhibit the activity of telomerase, which is a ribonucleoprotein enzyme presented in germ line cells, cancer-derived cell lines, and activated in 85–90% malignant tumors. For the achievement of anticancer drugs targeting G-quadruplexes, it is important to investigate influences of small ligands on the quadruplex-WC duplex equilibrium based on thermodynamic and kinetic characterizations.

*To whom correspondence should be addressed. Tel: +86 22 27890643; Fax: +86 22 27890643; Email: liwei@tju.edu.cn

Soy isoflavones, mainly including daidzein and genistein, together with their respective glycosidic conjugates of daidzin and genistin, have received considerable attention for their potential role in reducing the risk of head and neck, lung, breast and prostate cancers (29–34). For example, Kato *et al*. (35) reported that both genistin and daidzin possess anticancer effects at relatively early stages of prostate cancer development. Several studies indicated that genistein exerted antiproliferative influences on prostate cancer through the suppression of telomerase activity, which represses telomerase activity in prostate cancer cells not only by repressing hTERT transcriptional activity via c-Myc but also by posttranslational modification of hTERT via Akt (36,37). Guo *et al*. (38) reported that daidzein can affect human nonhormone-dependent cervical cancer cells in several ways, including cell growth, cell cycle and telomerase activity *in vitro*. Although several mechanisms for the in vitro anti-cancer effects of isoflavones compounds have been proposed, involving inhibition of protein tyrosine phosphorylation, inhibition of topoisomerases, induction of apoptosis and cell differentiation, inhibition of carcinogenesis and tumor promotion, suppression of telomerase activity, etc. (39,40), the main cellular target of isoflavone components remains elusive yet. The increasingly reported anticancer effects of isoflavones enlighten us to investigate molecular interactions between isoflavones and human telomeric G-rich sequences against their corresponding duplex.

In this article, we intensively studied the role of isoflavones including daidzein and genistein, and glycosidic daidzin and genistin on the structural competition of G-quadruplex d[$AG_3(T_2AG_3)_3$] and its related WC duplex d[$AG_3(T_2AG_3)_3$-$(C_3TA_2)_3C_3T$] in the presence of potassium by using circular dichroism (CD), ESI-MS, fluorescence quenching measurement, CD stopped-flow kinetic experiment, UV spectroscopy and molecular modeling methods. It is intriguing to find out that isoflavones can stabilize the G-quadruplex but destabilize the WC duplex and this discriminated interaction is intensified by molecular crowding environments. Stable complex between glycosidic isoflavones and the G-quadruplex is detected in a stoichiometric ratio of 1:1 and 2:1. Unfolding kinetics reflects that daidzin significantly decreases the unfolding rate of the G-quadruplex by 40.3% at the daidzin/DNA molar ratio of 1.0 in K^+, whereas in Na^+ the observed rate constant is reduced by about 12.0%. Furthermore, glycosidic daidzin induces a structural transition of the polymorphism G-quadruplex in K^+ into the antiparallel conformation. This is the first report on the interconversion between the duplex and the G-quadruplex as well as the transformation from the parallel to the antiparallel G-quadruplex induced by isoflavone constituents, which can provide important guidance to explore new clinic studies of isoflavone-based drugs.

MATERIALS AND METHODS

Chemicals and reagents

Oligonucleotides d[$AG_3(T_2AG_3)_3$] (denoted as AG22) and its complementary sequence CT22 d[$(C_3TA_2)_3C_3T$], d[$G_2CATAGTGCGTG_3CGT_2AGC$] and its complementary d[$GCTA_2CGC_3ACGCACTATGC_2$] were purchased from the Japanese Takara Bio (Dalian) with the purity > 98% measured by the reversed-phase high performance liquid chromatography (HPLC). Daidzin was purchased from Sigma with the purity higher than 97%, daidzein, genistein and genistin were purchased from Jiangxi Herbfine Hi-tech Co. with the purity > 98%. The structures of the small ligands used in this study are shown in Figure 1.

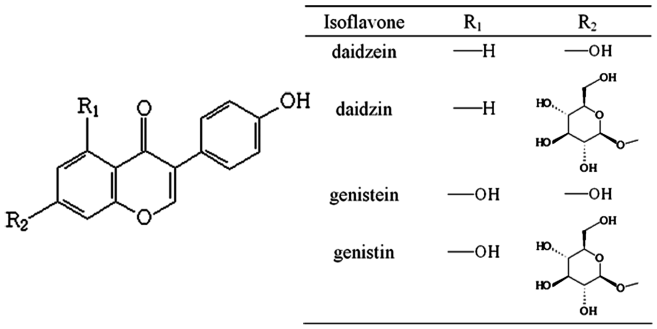

Figure 1. Structures of four main isoflavones, including daidzein, daidzin, genistein and genistin, respectively.

Circular dichroism

Circular dichroism (CD) experiments were carried out with a Jasco J-810 spectropolarimeter equipped with a Julabo temperature controller. All the CD spectra were measured for 50 μM total strand concentration of oligonucleotides in a 0.1 cm path-length cuvette with 90 mM Tris–Borate buffers containing 100 mM K^+ (pH 7.0). Each sample was scanned at least three times to get the average data curves from the wavelength of 200–350 nm. Thermal denaturation profiles were collected in units of millidegrees as a function of temperature. The heating rate was fixed at 1.0°C/min. The cell holding chamber was flushed with a constant stream of dry nitrogen gas to avoid water condensation on the cell exterior. All samples were annealed by heating the sample cuvette to 95°C for 10 min and then cooling to 4°C.

UV spectroscopy

UV melting profiles were performed on a Cary Varian UV/vis spectrophotometer equipped with a digital circulating water bath. The absorbance of oligonucleotides was monitored at 260 nm in a cuvette of 1 mm path-length with a heating rate of 1.0°C/min.

Mass spectrometry

Electrospray ionization mass spectrometry (ESI-MS) was utilized to investigate the binding stoichiometry of small molecule to G-quadruplex. Mass spectra were performed on a Thermo Finnigan LCQ Advantage in the negative ion mode. The experimental conditions were optimized to avoid denaturation of the quadruplex species: the heated capillary temperature of the electrospray source was set to 185°C, and a voltage on the heated capillary of −11 V.

Full scan MS spectra were recorded in a m/z range from 800 to 2000, and 50 scans were summed for each spectrum. The relative intensities of the free and bound DNA in the mass spectra are assumed to be proportional to the relative abundances of these species in solution.

Fluorescence titration

Fluorescence measurements were performed with a Cary Eclipse (Varian Ltd.) spectrofluorometer. The excitation wavelength was 249 nm for daidzin, 259 nm for genistin, respectively. The 2 μM isoflavone solutions containing 100 mM K^+ were titrated quantitatively with different concentrated DNA solutions at 20°C. The emission spectra were recorded from 450 nm to 600 nm.

CD stopped-flow kinetic measurement

CD stopped-flow kinetic measurements were performed using a JASCO J-810 spectropolarimeter equipped with SFM300 multi-mixing instruments (Bio-logic). After rapid mixing of 20 μM AG22 solution and 20 μM CT22 solution with total speed of 14 ml/s, the time course of the CD spectrum was recorded in units of millidegrees at the selected wavelength with a sample period of 500 ms. Data sets from at least four experiments performed under identical conditions were averaged and then fitted to single or double-exponential equations using Igor software (Wave-Metrics Inc., USA). In the presence of K^+, a double-exponential (Equation 1) fits the kinetic data well rather than a single-exponential one.

$$\Delta\theta = A_1 e^{-t/\Gamma_1} + A_2 e^{-t/\Gamma_2} + A_3 \quad \mathbf{1}$$

where Γ_1 and Γ_2 are the time constants of the decay and A_1 and A_2 are their respective amplitudes.

This double-exponential fitting kinetics is attributed to two serial processes depending on the individual rate of each step (41), from which the observed rate constant (k_{obs}) is generally calculated from the mean time constant (Γ) by Equation 2 as reported in Balasubramanian's studies (21,28,41).

$$1/\mathrm{k_{obs}} = \Gamma = \frac{A_1\Gamma_1 + A_2\Gamma_2}{A_1 + A_2} \quad \mathbf{2}$$

In the presence of Na^+, a single-exponential fitting is adopted to determine the observed rate constant according to Equation 3 (20), where k_{obs} equals to $1/\Gamma$.

$$\Delta\theta = A_1 e^{-t/\Gamma} + A_2 \quad \mathbf{3}$$

Molecular modeling

Three experimental structures are chosen as starting models, including the antiparallel basket-type NMR structure (PDB 143D), the parallel propeller-type X-ray structure (PDB 1KF1), and the mixed hybrid-type NMR structure deduced from a 26-nt DNA sequence (PDB 2HY9) through removal of two terminal adenines from each end of the 26-nt sequence (42,43). The AG22-CT22 duplex was built using the Biopolymer module within SYBYL6.92 (Tripos Inc., St Louis, MO, USA) with standard B-DNA geometries. They were subjected to molecular mechanics energy minimization (2000 steps) using Gasterger-Huckel charges, Tripos force field and conjugate gradient followed by dynamics (1 fs step, 50 ps at 298 K) and subsequent mechanics (minimization of time-averaged dynamics structure).

Ligand molecules including daidzin and genistin were built using Sketch module of the SYBYL6.92 and docked in their possible binding sites using DOCKING module of the Sybyl 6.92 package. In the case of the duplex, the binding sites were initially calculated and flexibly docked into the DNA secondary structure using the program DOCK5.0 (44), then according to the best scoring pose scored for electrostatic and van der Waals complementarity, we placed the ligand molecules in the corresponding position using Sybyl 6.92 followed by minimization. Relative binding energy (E_{bind}) was calculated according to equation $E_{bind} = E_{complex} - E_{receptor} - E_{ligand}$, where $E_{complex}$ denotes the total energy of the DNA–ligand complex, $E_{receptor}$ and E_{ligand} is the energy of the G-quadruplex DNA and the small molecules of daidzin or genistin, respectively.

RESULTS

Circular dichroism and thermal denaturation: isoflavones increase relative stability of human telomeric G-quadruplex against its related duplex

Influences of isoflavones including daidzin, genistin, daidzein and genistein on the conformation of human telomeric oligonucleotide $d[AG_3(T_2AG_3)_3]$ (AG22) and its equimolar mixture with the complementary sequence $d[(C_3TA_2)_3C_3T]$ (CT22) were characterized by using CD spectroscopy in the presence of 100 mM K^+, respectively. As shown in Figure 2a and b, CD spectra of $d[AG_3(T_2AG_3)_3]$ exhibit a positive peak around 290 nm, a trough at 238 nm and an obvious shoulder peak around 260 nm, which results from the highly polymorphic quadruplex of human telomeric DNA in K^+ solution (45–48). Addition of either daidzin or genistin results in stronger intensities of both the positive and the negative peak, whereas adding aglycosidic daidzein or genistein induces little changes of CD spectra of $d[AG_3(T_2AG_3)_3]$ (Figure 2c and d). In the case of double-stranded AG22-CT22, neither of these four isoflavones induce obvious changes in CD spectra (see Supplementary Figure S1).

According to CD thermal denaturation profiles of AG22 and AG22-CT22 under different concentration of isoflavones in the presence of 100 mM K^+ (Supplementary Figures S2 and S3), variation values of melting temperatures (ΔT_m) respective for AG22 and AG22-CT22 induced by isoflavones respectively are displayed in Figure 3a and b. It is intriguing to find that addition of glycosidic daidzin or genistin makes the T_m value of G-quadruplex increased but the T_m of the corresponding duplex decreased (Figure 3a), especially as the daidzin/DNA molar ratio equals to 0.5, the T_m value of G-quadruplex AG22 increases to 78.0°C that

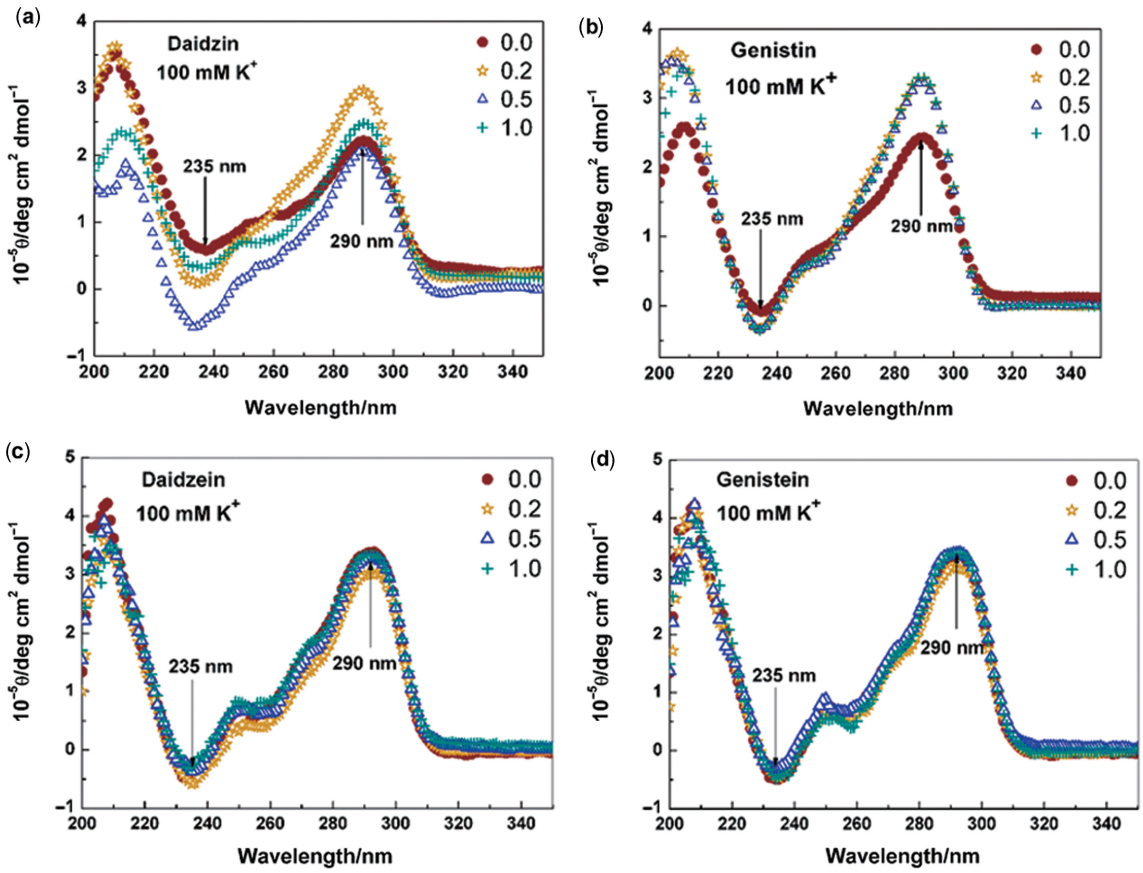

Figure 2. CD spectra of 50 μM AG22 in the presence of 100 mM K^+ with different concentration of daidzin (**a**), genistin (**b**), daidzein (**c**) and genistein (**d**) in 90 mM TB buffer (pH = 7.0) at 20°C. The molar ratio of isoflavone/AG22 is 0.0, 0.2, 0.5 and 1.0, respectively.

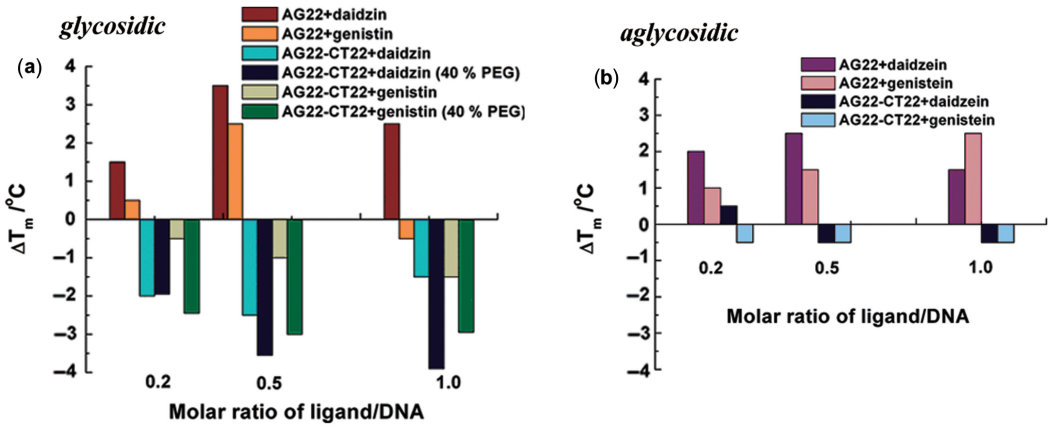

Figure 3. Variation of melting temperatures (ΔT_m) for both AG22 and AG22-CT22 in the presence of 100 mM K^+ under different concentration of glycosidic daidzin and genistin (**a**) and aglycosidic daidzein and genistein (**b**) in 90 mM TB buffer (pH = 7.0). The SD for melting temperature is <0.28°C.

closely approximates to the T_m of AG22-CT22 (78.5°C). While addition of the aglycosidic daidzein and genistein, similar influences are observed on T_m values of the G-quadruplex and of the duplex, just like their glycosidic counterpart but with smaller variation amplitude (Figure 3b).

Molecular crowding conditions are considered to be beneficial to the structural competition of the G-quadruplex against the duplex (49–52). In order to study the effects of molecular crowding conditions on the structural competition of G-quadruplex and the duplex, UV denaturation profiles were measured for the AG22-CT22 duplex under 40% (w/v) PEG200 with 100 mM K^+ and in the presence of different concentrations of daidzin or genistin (Supplementary Figure S4). Both daidzin and genistin exhibit stronger destabilization effects on the AG22-CT22 with maximum decreasing ΔT_m of 4.0°C and 3.0°C, respectively under molecular crowding

conditions, compared with those without crowding agent (Figure 3a). In the case of single-stranded AG22 under molecular crowding conditions in the presence of K^+, it is hard to investigate the effects of small ligands on the thermal stability of G-quadruplex as AG22 exhibits an unusual stability. However, in the presence of Na^+, crowding conditions made the transition temperature of AG22 increased by 13.0°C at the daidzin/AG22 ratio of 1.0 (53).

As a control, denaturation profiles were performed for the nonquadruplex-forming duplex d[G_2CATAGTGCG TG_3CGT$_2$AGC]-d[GCTA$_2$CGC$_3$ACGCACTATGC$_2$] in the presence of K^+ with daidzin or genistin added. Genistin exhibits destabilization effect on this duplex with maximum decreasing ΔT_m of 2.6°C at the ligand/duplex molar ratio of 0.5, meanwhile daidzin shows a little destabilization effect with decreasing ΔT_m of 0.4°C (Supplementary Figure S4). These results illuminate that glycosidic isoflavones destabilize the Watson–Crick duplexes of both G-rich and nonquadruplex-forming oligonucleotides.

Electrospray mass spectrometry: stoichiometry of isoflavones and G-quadruplex

ESI-MS spectra is adopted to determine the stoichiometry and affinity of isoflavones with AG22 quadruplex in the presence of 150 mM monovalent ammonia ions that are popular substitutes for Na^+ and K^+ in the ESI-MS measurement (54). Compared with the mass spectra of AG22 alone illustrated in Figure 4a, a mixture of 1:1 and 2:1 genistin–AG22 complexes are detected in the case of glycosidic genistin (Figure 4c), while no ligand–AG22 complex is observed with aglycosidic genistein added (Figure 4b). Combining with the MS spectra containing daidzin and daidzein (Supplementary Figure S5), it suggests that glycosidic isoflavones can form adducts with AG22 in a stoichiometric ratio of 1:1 and 2:1, whereas no species with high abundance are related to stable complex between aglycosidic isoflavones and AG22. These ESI-MS results disclose different binding modes of glycosidic isoflavones from their aglycosidic counterparts. To make semiquantitative comparisons between glycosidic daidzin and genistin, the affinity of isoflavones for AG22 G-quadruplex is characterized by the concentration of bound ligand per G-quartet, which was fully described in Mergny's studies (54). The amount of isoflavone bound to AG22 is determined as 0.901 μM for daidzin per G-quartet, which is higher than that value of genistin (0.686 μM). Thus, daidzin has higher binding affinity to the G-quadruplex than genistin in the presence of ammonia ions where AG22 adopts antiparallel conformation.

Fluorescence titration: interactions between isoflavones and G-quadruplex

Fluorescence emission spectra for mixtures of each glycosidic isoflavone and AG22 were measured in order to

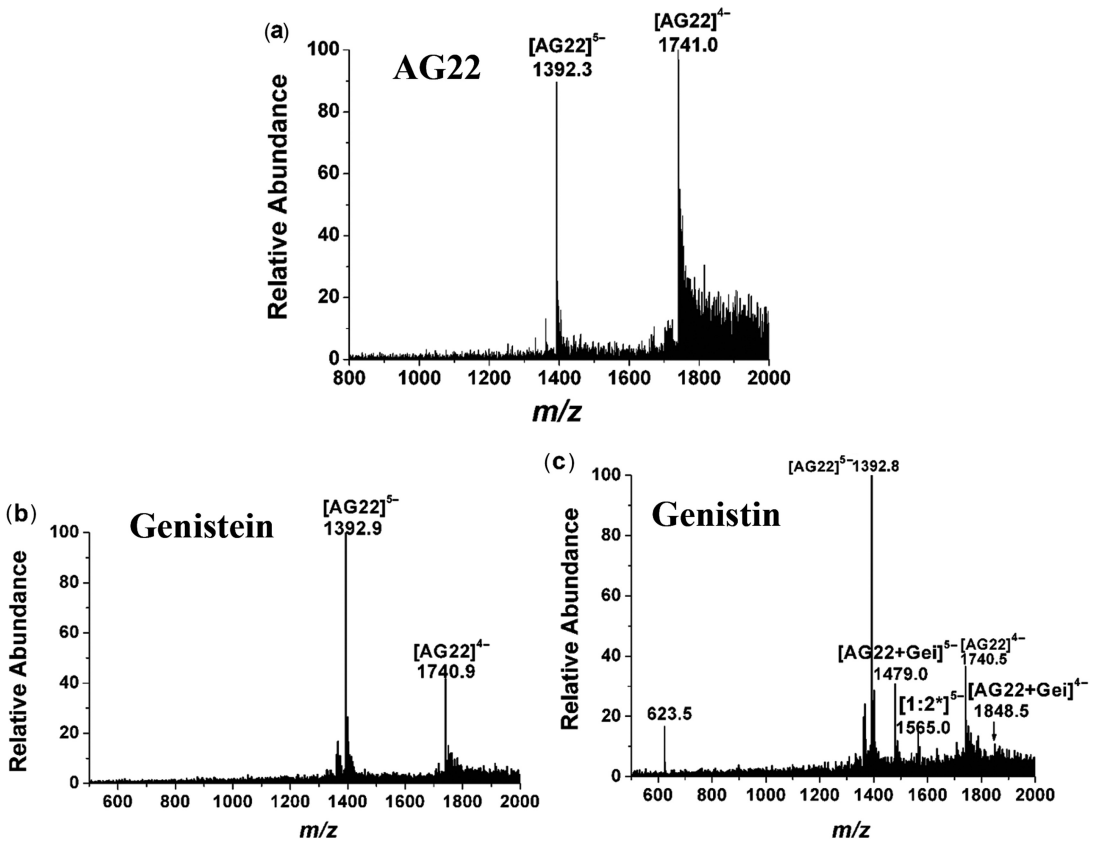

Figure 4. ESI-MS spectra of 5 μM AG22 alone (**a**), and its mixtures with 50 μM genistein (**b**), or genistin (**c**) in the presence of 150 mM NH_4OAc buffer (pH = 7.0).

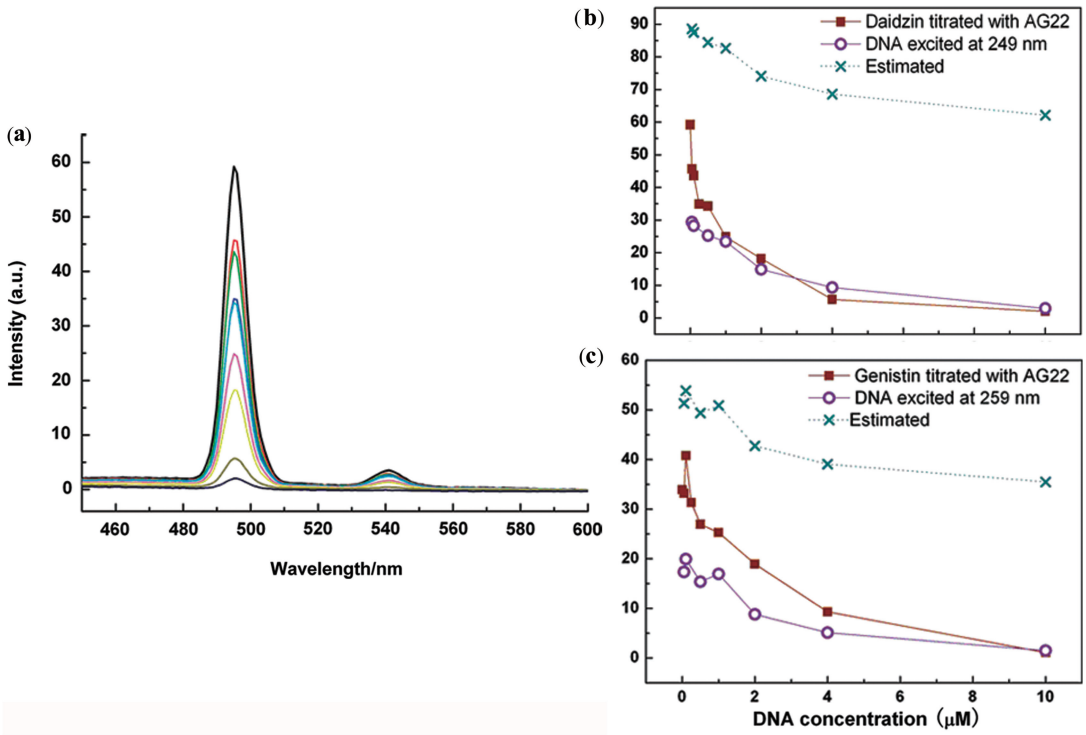

Figure 5. (**a**) Fluorescence spectra of 2 μM daidzin in 100 mM K^+, 90 mM TB buffer (pH = 7.0) titrated with different concentrations of AG22 at 20°C; the plots of observed maximal fluorescence intensity of daidzin at 495 nm (**b**) and genisin at 520 nm (**c**) versus concentrations of AG22.

disclose whether or not collisional and static quenching occur among isoflavone and DNA molecules. Figure 5a shows representative fluorescence spectra of daidzin titrated with different amount of AG22 in the presence of K^+. Fluorescence intensity of daidzin at 495 nm gradually decreases as the concentration of AG22 increasing. Similar tendency of fluorescence spectra is observed when genistin is titrated by DNA solution in the presence of 100 mM K^+ (Supplementary Figure S6). The plot of maximal fluorescence intensity versus DNA concentration exhibits a nonlinear curve in the presence of K^+ for either daidzin or genistin, as indicated by solid lines in Figure 5b and c, respectively.

Because the excitation wavelength of either daidzin or genistin is overlapped with the distinct wavelength of DNA absorption at 260 nm, there exist inner filter effects in the related fluorescence quenching system (55). In order to assess the inner filter effects, the fluorescence spectra of DNA alone with the titration concentrations were measured in the absence of isoflavone molecules, excited at the wavelength of 249 nm or 259 nm respectively. As illustrated by dash lines in Figure 5b and c, intensity of estimated emission spectra which calculated by summation of fluorescence intensity of each concentrated AG22 and that of individual daidzin or genistin is greatly stronger than that of observed fluorescence quenching intensity, especially at low molar ratio of ligand/DNA (<2.0). Although it is hard to correct the inner filter effect of the complicated system and the binding constants can not be determined quantitatively, it suggests the existence of static quenching between DNA and the ligand of daidzin or genistin, which indicates complex formed and is consistent with the above ESI-MS results.

Stopped-flow kinetic measurements: effects of isoflavones on the decomposition of G-quadruplex

To investigate the influences of glycosidic isoflavones on the structural competition between the G-quadruplex and the WC duplex, we collected kinetic traces under the ligand/DNA molar ratio of 0.5 and 1.0 by CD stopped-flow experiments in the presence of 100 mM K^+ as well as those without small ligands. Figure 6 displays kinetic time courses recorded respectively at 290 nm and at 265 nm upon mixing equimolar AG22 and CT22 in 100 mM K^+ without small ligands, and in the presence of daidzin or genistin with the ligand/DNA molar ratio of 1.0. A double-exponential equation was found to fit the kinetic time courses well rather than a single-exponential one. In the absence of small ligands, the observed rate constant ($k_{obs290\,nm}$) determined using the kinetic traces at 290 nm equals to $(4.77 \pm 0.92) \times 10^{-3}\,s^{-1}$ which reflects the unfolding rate of the antiparallel quadruplex in the presence of K^+, while the observed rate constant ($k_{obs265\,nm}$) determined at 265 nm is $(3.25 \pm 0.60) \times 10^{-3}\,s^{-1}$ that corresponds the formation rate of the duplex. In previous work, Balasubramanian and coworkers (18) determined the unfolding rate of 21-nt $[(G_3T_2A)_3G_3]$ as $0.002\,s^{-1}$ using fluorescence resonance energy transfer in the presence of 100 mM K^+ at 37°C, which is in the same order of $k_{obs290\,nm}$ obtained here.

Upon addition of glycosidic isoflavones, it is observed that the value of $k_{obs290\,nm}$ decreases, whereas the value of

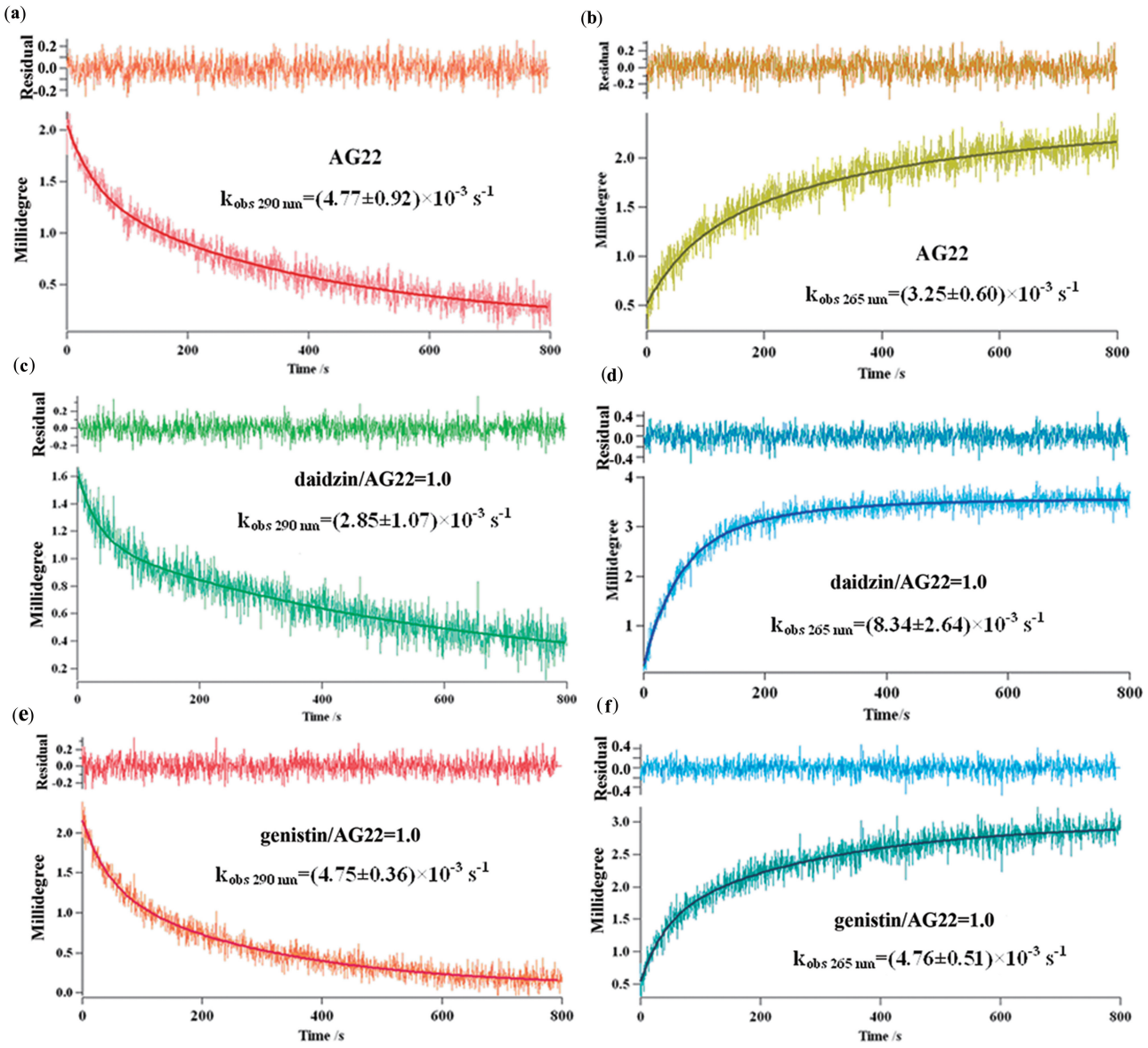

Figure 6. Kinetic time courses upon mixing 20 μM AG22 and CT22 with the same concentration in 100 mM K^+ (90 mM TB buffer) at 37°C without small ligands, recorded at 290 nm (**a**) and at 265 nm (**b**); and in the presence of 20 μM daidzin [recorded at 290 nm (**c**) and at 265 nm (**d**)]; or in the presence of 20 μM genistin [recorded at 290 nm (**e**) and at 265 nm (**f**)].

$k_{obs265\,nm}$ increases. Under the ligand/DNA molar ratio of 1.0, addition of daidzin makes $k_{obs290\,nm}$ decreased to $(2.85\pm1.07)\times10^{-3}\,s^{-1}$ but $k_{obs265\,nm}$ increased significantly to $(8.34\pm2.64)\times10^{-3}\,s^{-1}$ (Figure 6c and d), while genistin makes $k_{obs290\,nm}$ decreased slightly but $k_{obs265\,nm}$ increased to $(4.76\pm0.51)\times10^{-3}\,s^{-1}$ (Figure 6e and f). In the case of ligand/AG22 molar ratio of 0.5, the kinetic time courses can also be fitted well using the double-exponential equation (Supplementary Figure S7) and the observed rate constants indicate the variation tendency similar to that under the ligand/AG22 ratio of 1.0, especially for daidzin. Table 1 lists values of $k_{obs290\,nm}$ and $k_{obs265\,nm}$ as the ligand/AG22 ratio increases from 0.5 to 1.0. It is noteworthy that the G-quadruplex unfolding rate $k_{obs290\,nm}$ decreases by a fraction of 34.8%, whereas the duplex formation rate $k_{obs265\,nm}$ increases by 137.2% as the daidzin/DNA molar ratio increases to 0.5. In the case of genistin with the ratio of 0.5, the $k_{obs290\,nm}$ decreases by 9.2%, while $k_{obs265\,nm}$ increases by 22.8%. Previous work suggests that the G-quadruplex unfolding experiences two steps, where initial unfolding of G-quadruplex is the rate-determining step followed by a fast association of duplex (41). Therefore, the amplitude of $k_{obs290\,nm}$ decreasing should be approximate to that of $k_{obs265\,nm}$ increasing.

In order to deduce the reason that the strange inconsistent variation of $k_{obs290\,nm}$ against $k_{obs265\,nm}$, CD stopped-flow experiments were also performed in the presence of Na^+ with the molar ratio daidzin/AG22 of 0.0 and 1.0, respectively. As illustrated in Figure 7, the kinetic time

courses are fitted well using the single-exponential equation. In the absence of daidzin, the $k_{obs295\,nm}$ is determined as $0.101 \pm 0.008\,s^{-1}$ and $k_{obs265\,nm}$ as $0.0841 \pm 0.0019\,s^{-1}$. Whereas addition of equimolar daidzin makes the $k_{obs295\,nm}$ decreased by 12.0% and $k_{obs265\,nm}$ decreased by 9.3%, respectively, which is in accordance with the two-step unfolding of G-quadruplex (20). It is known that 22-nt d[$AG_3(T_2AG_3)_3$] in K^+ solution is most likely present as a mixture of two or more conformations, such as a hybrid-type and basket antiparallel topologies (45,46), whereas AG22 in Na^+ solution adopts antiparallel basket type conformation characterized by NMR (56). The existence of hybrid-type conformation induces a shoulder peak around 265 nm in the CD spectra besides the peak at 290 nm, and both of these peaks decrease as quadruplex unfolding (Supplementary Figure S8a). Consequently, the change of CD intensity at 265 nm recorded in these kinetic courses reflects not only the duplex association but also the dissociation of hybrid-type G-quadruplex. Therefore, the obvious augment of $k_{obs265\,nm}$ induced by daidzin in the presence of K^+ is attributed to a structural transformation from hybrid-type to antiparallel conformation, i.e. molecular interaction of daidzin is preferential to stabilize the antiparallel G-quadruplex.

Table 1. Observed rate constants obtained by double-exponential fit in the presence of K^+ and different concentrated ligands at 37°C

Ligand	Ligand/ AG22	Measured at 290 nm (s^{-1})	measured at 265 nm (s^{-1})
None	0	$(4.77 \pm 0.92) \times 10^{-3}$	$(3.25 \pm 0.60) \times 10^{-3}$
Daidzin	0.5	$(3.11 \pm 0.51) \times 10^{-3}$	$(7.71 \pm 1.70) \times 10^{-3}$
	1.0	$(2.85 \pm 1.07) \times 10^{-3}$	$(8.34 \pm 2.64) \times 10^{-3}$
Genistin	0.5	$(4.33 \pm 0.51) \times 10^{-3}$	$(3.99 \pm 0.58) \times 10^{-3}$
	1.0	$(4.75 \pm 0.36) \times 10^{-3}$	$(4.76 \pm 0.51) \times 10^{-3}$

DISCUSSION

Glycosidic isoflavones stabilize the G-quadruplex but destabilize the duplex

According to CD spectra (Figure 2), thermal denaturation (Figure 3), MS spectra (Figure 4) and fluorescence quenching results (Figure 5), it is reasonable to conclude that glycosidic isoflavones can stabilize AG22 quadruplex but destabilize its related duplex and form stable comlpexes with AG22 quadruplex in a stoichiometric ratio of 1:1 and 2:1. In order to deduce the molecular mechanism of G-quadruplex recognition by glycosidic isoflavones, molecular simulation is adopted to study the binding modes of isoflavones with AG22 G-quadruplex.

It is well known that the conformation of human telomeric G-quadruplex in K^+ is polymorphic and greatly depends on the sequence (45–48). CD spectra indicate that conformation of AG22 in K^+ solution is complicated and distinct from hybrid-type quadruplex alone

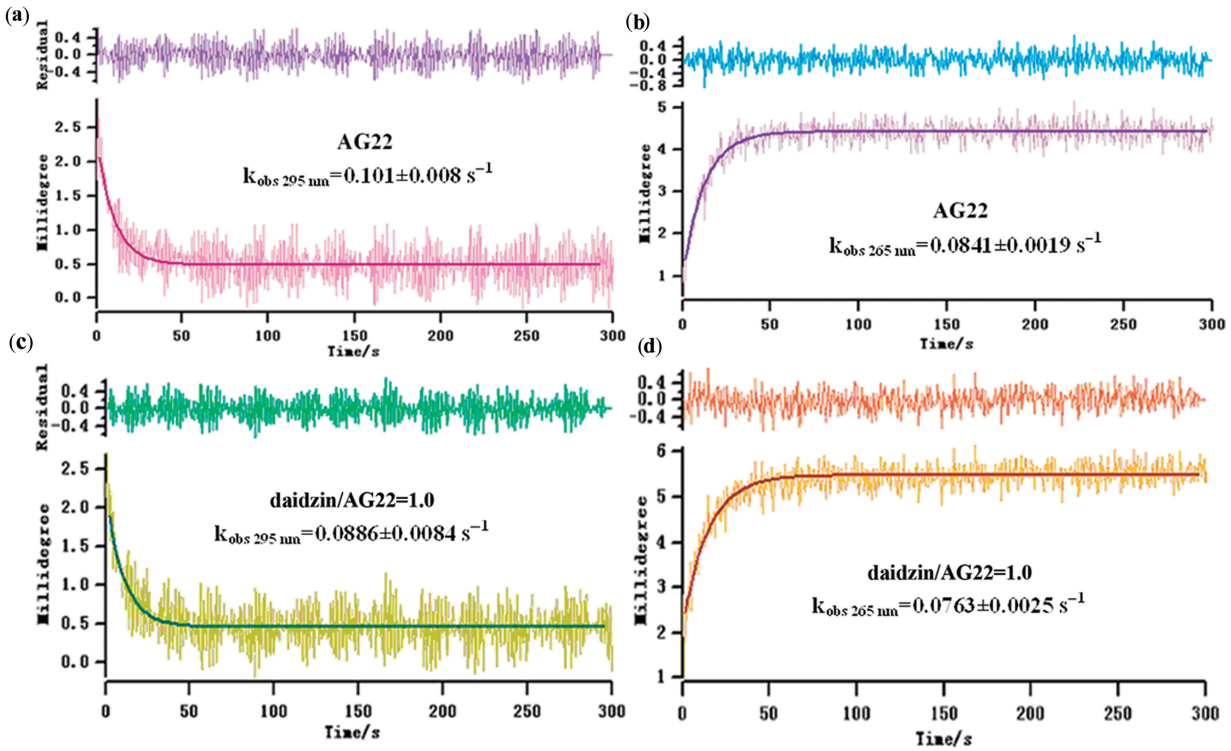

Figure 7. Kinetic time courses obtained upon mixing 20 μM AG22 and CT22 with the same concentration in 100 mM Na^+ (90 mM TB buffer) at 40°C without small ligands, recorded at 295 nm (**a**) and at 265 nm (**b**); and in the presence of 20 μM daidzin [recorded at 295 nm (**c**) and at 265 nm (**d**)].

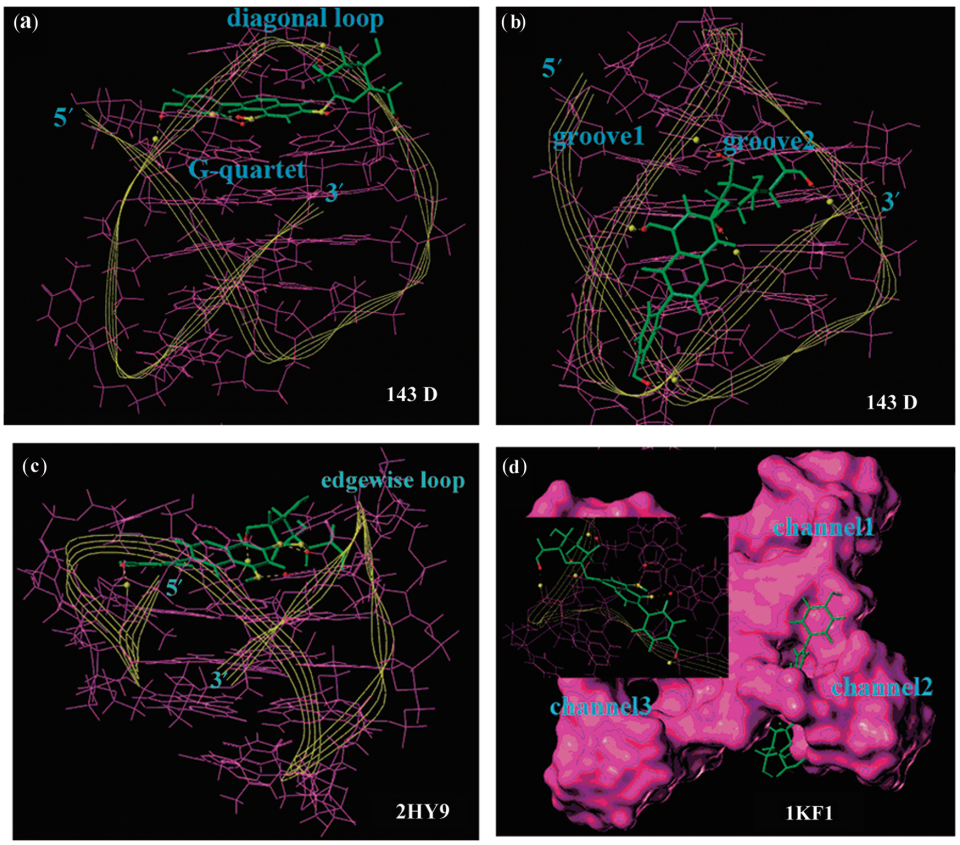

Figure 8. Models of quadruplex–genistin complexes with different binding sites: (**a**) genistin located between 5′ G-quartet and the diagonal loop of the antiparallel 143D with six hydrogen bondings, O36H-Genistin...O294-G10, O32H-Genistin...O359-T12, O25-Genistin...N405H-A13, O18-Genistin...N14H-A1, O18H-Genistin...N15-A1, O12H-Genistin...O65-G3, for instance, O36H-Genistin...O294-G10 means that the oxygen atom No. 294 (O294) in the guanine base No.10 (G10) of the AG22 forms hydrogen bonding with the hydrogen atom connected with the oxygen atom No. 36 (O36) of genistin; (**b**) Genistin located in the groove2 of the antiparallel 143D with five hydrogen bondings, O32H-Genistin...O618-G20, O36-Genistin...O651-G21, O33H-Genistin...O456-G15, O18H-Genistin...O489-G16, O12H-Genistin...O585-A19; (**c**) Genistin located in 5′ G-quartet of the modified hybrid-type 2HY9 with five hydrogen bondings, O12H-Genistin...O38-G2, O18-Genistin...N601H-A19, O25-Genistin...N535H-T17, O27-Genistin...N535H-T17, O32H-Genistin...O261-G9; (**d**) Genistin located in the channel2 of parallel 1KF1 and inset image is the magnified view which shows six hydrogen bondings, O36H-Genistin...O253-A13, O32H-Genistin...O297-G15, O33H-Genistin...O214-T11, O12H-Genistin...O169-G9, O18-Genistin...N187H-G9, O24-Genistin...N165H-G8. The small red points indicate donors of hydrogen bonding and the large yellow points are acceptors.

(Supplementary Figure S8b). Therefore, three experimental structures are chosen as starting models in our simulations, including antiparallel basket-type G-quadruplex (PDB 143D), hybrid-type G-quadruplex (PDB 2HY9) and parallel propeller-type G-quadruplex (PDB 1KF1) separately (43). As shown in Figure 8, preferable binding sites of genistin are respectively obtained to be 5′ G-quartet plane (with a diagonal loop) and groove2 (between the 3′-end and residues 14–17) for 143D, 5′-terminal G-quartet plane (with a edgewise loop) for 2HY9, and channel 2 (T11T12A13 loop and G-tetrads) for 1KF1. The stable hydrogen bondings formed between genistin and G-quadruplex are also illustrated in Figure 8. In the case of daidzin, it is preferable to form a stable complex with 143D through π–π conjugacy interactions and hydrogen bondings docked between the diagonal loop and 5′ G-quartet plane (53). The 5′-terminal G-quartet plane in 2HY9 is also the preferable binding site for daidzin with five hydrogen bondings formed (Supplementary Figure S9a). In combination with thermal stability of G-quadruplex in the presence of isoflavones, it is attributed to these stable hydrogen bondings and π–π conjugacy interactions that make the G-quadruplex stabilized by genistin or daidzin.

In the case of the WC-duplex AG22-CT22, flexibly docking calculations suggest that genistin interacts preferably with T12A13G14G15 in the minor groove with three hydrogen bondings and daidzin binds to G10T11T12A13 in the minor groove with two hydrogen bondings (Supplementary Figure S10). Comparing the plane angles and hydrogen bonding distributions of base pairs in duplex alone with those in the duplex–ligand complex through statistical analysis, it is reflected that interactions of genistin or daidzin result in the increments of average plane angles as well as stretching distances of hydrogen bondings of base pairs in the AG22-CT22 duplex (Figure 9). These results illuminate that the destabilization of WC duplex induced by glycosidic isoflavones is due to the weakening effects of genistin and daidzin on the hydrogen bondings between base pairs.

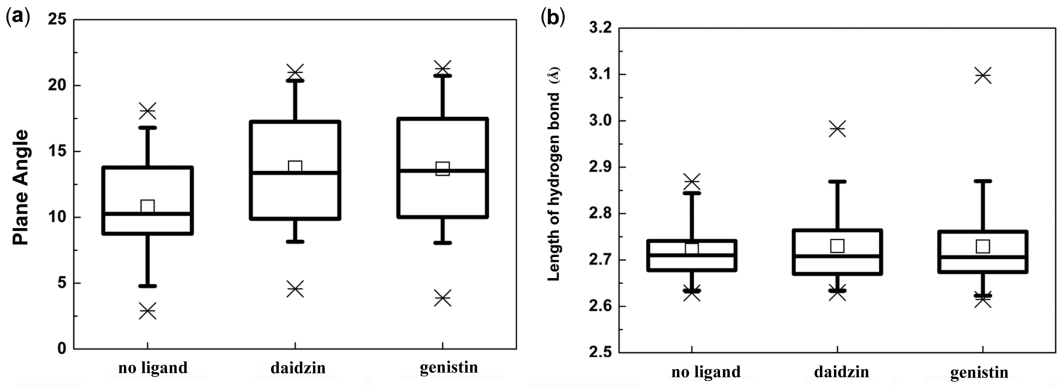

Figure 9. Statistical graphs of plane angles (**a**) and hydrogen bondings distributions (**b**) of base pairs in AG22-CT22 and the duplex–ligand complex. Boxes include 25–75% of the values. The vertical lines begin at 5th percentile and end at 95th percentile and the small square represents the average value.

Glycosidic daidzin modulates the quadruplex–duplex competition and the conformational transformation of telomeric G-quadruplex

Kinetic courses recorded by CD stopped-flow measurements (Figures 6 and 7, Table 1) illuminate that daidzin can significantly delay the unfolding process of AG22 G-quadruplex and induce a structural transformation from mixed antiparallel/parallel to antiparallel quadruplex, whereas gensitin shows slight influence compared with daidzin.

CD stopped-flow measurements here indicate that daidzin makes the observed rate constant reduced by about 12.0% at the daidzin/AG22 molar ratio of 1.0 in the presence of Na^+. This amplitude of $k_{obs295\,nm}$ variation is comparable to Balasubramanian *et al.*'s (28) work on a hemicyanine-peptide ligand to the quadruplex unfolding which showed that the observed rate constant in the hybridization reaction between G-quadruplex and its complementary C-rich strand was decreased by 38.4% and 68.6% at a ligand/quadruplex molar ratio of 500 and 5000 at 20°C in Na^+ solution, respectively. In the presence of K^+ daidzin makes the dissociation rate of quadruplex ($k_{obs290\,nm}$) decreased by 34.8% and 40.3% at the daidzin/DNA molar ratio of 0.5 and 1.0, respectively. Similarly, Kumar and Maiti (21) reported that TMPyP4, a small quadruplex-interactive drug, can induce a significant decrease in the observed rate constant of the hybridization reaction between G-quadruplex and its complementary strand by 28.0% in the presence of K^+ at a TMPyP4/quadruplex molar ratio of 5 at 20°C. According to molecular modeling results, daidzin prefers л–л stacking with the antiparallel G-tetraplex as well as hydrogen bondings with the bases in the diagonal loop, which attributes to apparent retard of the quadruplex dissociation. Genistin is preferable to bind in the groove region for the antiparallel quadruplex besides stacking on 5′-terminal G-quartet, which contributes less to inhibit the unfolding process.

Intriguingly, kinetic measurements disclose that significant increment of $k_{obs265\,nm}$ in K^+ is due to the transformation from hybrid-type to antiparallel G-quadruplex induced by glycosidic daidzin and genistin. Similar with the selective stabilization of telomestatin and TMPyP4 on the antiparallel basket conformation of 21-nt $d[G_3(T_2AG_3)_3]$ in K^+ solution (46), it is noticeable that glycosidic isoflavones can modulate the type of telomeric G-quadruplex structures beyond thermal stabilization of these structures.

Biological implications of interaction of isoflavone constituents with G-quadruplex DNA

The human telomeric G-quadruplex is being increasingly considered as a potential molecular target for developing novel anticancer agents (57,58), because stabilization of G-quadruplex by small molecules is probably one potential mechanism to decrease telomerase efficiency. Among plenty of quadruplex-selective ligands as listed in Table 2, some ligands including macrocyclic oligoamides, nickel salen complexes and oxazole-based peptide macrocycles result in obvious increase of the G-quadruplex stability, with no effects on the transition temperature of the duplex. The others involving the platinum supramolecular square and BRACO-19 increase the transition temperature not only of G-quadruplex but also of the duplex. To our knowledge, the opposite interaction of glycosidic isoflavones with G-quadruplex against the WC-duplex presented here is the first report on the quadruplex-targeting ligands that can reduce the stability of its related duplex.

Along with increasing epidemiological and experimental studies on the anticancer effects of soy isoflavones, it is suggested that molecular interactions between isoflavones and human telomeric G-rich DNA are promisingly associate with the suppression of telomerase activity. Polkowski et al reported that the lipophilic glycosidic derivatives of genistein were significantly active and exhibited different mode of action in comparison to genistein against human cancer cell lines (59). Yanagihara *et al.*'s (60) studies showed that among seven isoflavone derivatives, biochanin A and genistein can inhibit the cell growth of stomach cancer cell lines in vitro through activation of a signal transduction pathway for apoptosis. Jing *et al.* (61) reported that the potency of natural isoflavones on cell growth inhibition and differentiation induction is

Table 2. Effects of quadruplex-targeting ligands on the transition temperature of 200 nM G-quadruplex and duplex determined by FRET (the ligand concentration is 1 μM except the platinum square of 0.75 μM)

The ligand to G-quadruplex	ΔT_m/°C	
	G-quadruplex	Duplex
Platinum supramolecular square (23)	34.5	12.1
Macrocyclic oligoamides (24)	33.8	0.0
Nickel Salen complex (25)	33.2	0.0
Telomestatin (24)	30.3	0.0
BRACO-19 (25)	27.5	14.5
Helical oligoamide (24)	23.7	0.7
Trisubstituted isoalloxazines (11)	7.0–19.3	0.0
Oxazole-based peptide macrocycles (26)	4.5–6.4	0.0

dependent upon the isoflavone structure and hydroxyl groups. It is consistent with the results obtained here, i.e. glycoside plays an important role in the relationship between isoflavones and telomeric DNA secondary structures. Here, both thermodynamic and kinetic results illuminate that daidzin and genistin exhibit differential recognition on the G-quadruplex DNA, and distinct regulation on the structural competition or conformational transformation in human telomeric DNA, which indicate that these constituents exert their anticancer effects in potentially different molecular action pathway *in vivo*.

SUPPLEMENTARY DATA

Supplementary Data are available at NAR Online.

FUNDING

NSFC (No. 20576090, 20776102, 20836005); the NCET.

REFERENCES

1. Arthanari,H. and Bolton,P.H. (2001) Functional and dysfunctional roles of quadruplex DNA in cells. *Chem. Biol.*, **8**, 221–230.
2. Keniry,M.A. (2001) Quadruplex structures in nucleic acids. *Biopolymers*, **56**, 123–146.
3. Hammond-Kosack,M.C.U., Dobrinski,B., Lurz,R., Docherty,K. and Kilpatrick,M.W. (1992) The human insulin gene linked polymorphic region exhibits an altered DNA structure. *Nucleic Acids Res.*, **20**, 231–236.
4. Yafe,A., Etzioni,S., Weisman-Shomer,P. and Fry,M. (2005) Formation and properties of hairpin and tetraplex structures of guanine-rich regulatory sequences of muscle-specific genes. *Nucleic Acids Res.*, **33**, 2887–2900.
5. Siddiqui-Jain,A., Grand,C.L., Bearss,D.J. and Hurley,L.H. (2002) Direct evidence for a G-quadruplex in a promoter region and its targeting with a small molecule to repress c-MYC transcription. *Proc. Natl Acad. Sci. USA*, **99**, 11593–11598.
6. Fernando,H., Reszka,A.P., Huppert,J., Ladame,S., Rankin,S., Venkitaraman,A.R., Neidle,S. and Balasubramanian,S. (2006) A conserved quadruplex motif located in a transcription activation site of the human c-kit oncogene. *Biochemistry*, **45**, 7854–7860.
7. Dexheimer,T.S., Sun,D. and Hurley,L.H. (2006) Deconvoluting the structural and drug-recognition complexity of the G-quadruplex-forming region upstream of the bcl-2 P1 promoter. *J. Am. Chem. Soc.*, **128**, 5404–5415.
8. Sun,D., Guo,K., Rusche,J.J. and Hurley,L.H. (2005) Facilitation of a structural transition in the polypurine/polypyrimidine tract within the proximal promoter region of the human VEGF gene by the presence of potassium and G-quadruplex-interactive agents. *Nucleic Acids Res.*, **33**, 6070–6080.
9. Guo,K., Pourpak,A., Beetz-Rogers,K., Gokhale,V., Sun,D. and Hurley,L.H. (2007) Formation of pseudosymmetrical G-quadruplex and i-motif structures in the proximal promoter region of the RET oncogene. *J. Am. Chem. Soc.*, **129**, 10220–10228.
10. Cogoi,S. and Xodo,L.E. (2006) G-quadruplex formation within the promoter of the KRAS proto-oncogene and its effect on transcription. *Nucleic Acids Res.*, **34**, 2536–2549.
11. Bejugam,M., Sewitz,S., Shirude,P.S., Rodriguez,R., Shahid,R. and Balasubramanian,S. (2007) Trisubstituted isoalloxazines as a new class of G-quadruplex binding ligands: small molecule regulation of c-kit oncogene expression. *J. Am. Chem. Soc.*, **129**, 12926–12927.
12. Sun,D., Liu,W.-J., Guo,K., Rusche,J.J., Ebbinghaus,S., Gokhale,V. and Hurley,L.H. (2008) Proximal promoter region of the human vascular endothelial growth factor gene has a G-quadruplex structure which can be targeted by G-quadruplex-interactive agents. *Mol. Cancer Ther.*, **7**, 880–889.
13. Qin,Y., Rezler,E.M., Gokhale,V., Sun,D. and Hurley,L.H. (2007) Characterization of the G-quadruplexes in the duplex nuclease hypersensitive element of the PDGF-A promoter and modulation of PDGF-A promoter activity by TMPyP4. *Nucleic Acids Res.*, **35**, 7698–7713.
14. Bourdoncle,A., Estévez Torres,A., Gosse,C., Lacroix,L., Vekhoff,P., Le Saux,T., Jullien,L. and Mergny,J.L. (2006) Quadruplex-based molecular beacons as tunable DNA probes. *J. Am. Chem. Soc.*, **128**, 11094–11105.
15. Miyoshi,D., Inoue,M. and Sugimoto,N. (2006) DNA logic gates based on structural polymorphism of telomere DNA molecules responding to chemical input signals. *Angew. Chem. Int. Ed.*, **45**, 7716–7719.
16. Alberti,P. and Mergny,J.-L. (2003) DNA duplex-quadruplex exchange as the basis for ananomolecular machine. *Proc. Natl Acad. Sci. USA*, **100**, 1569–1573.
17. Kumar,N., Sahoo,B., Varun,K.A.S., Maiti,S. and Maiti,S. (2008) Effect of loop length variation on quadruplex-Watson Crick duplex competition. *Nucleic Acids Res.*, **36**, 4433–4442.
18. Ying,L., Green,J.J., Li,H., Klenerman,D. and Balasubramanian,S. (2003) Studies on the structure and dynamics of the human telomeric G-quadruplex by single-molecule fluorescence resonance energy transfer. *Proc. Natl Acad. Sci. USA*, **100**, 14629–14634.
19. Li,W., Wu,P., Ohmichi,T. and Sugimoto,N. (2002) Characterization and thermodynamic properties of quadruplex/duplex competition. *FEBS Lett.*, **526**, 77–81.
20. Li,W., Miyoshi,D., Nakano,S.-I. and Sugimoto,N. (2003) Structural competition involving G-quadruplex DNA and its complement. *Biochemistry*, **42**, 11736–11744.
21. Kumar,N. and Maiti,S. (2005) The effect of osmolytes and small molecule on Quadruplex-WC duplex equilibrium: a fluorescence resonance energy transfer study. *Nucleic Acids Res.*, **33**, 6723–6732.
22. Kim,M.-Y., Vankayalapati,H., Shin-ya,K., Wierzba,K. and Hurley,L.H. (2002) Telomestatin, a potent telomerase inhibitor that interacts quite specifically with the human telomeric intramolecular G-quadruplex. *J. Am. Chem. Soc.*, **124**, 2098–2099.
23. Kieltyka,R., Englebienne,P., Fakhoury,J., Autexier,C., Moitessier,N. and Sleiman,H.F. (2008) A platinum supramolecular square as an effective G-quadruplex binder and telomerase inhibitor. *J. Am. Chem. Soc.*, **130**, 10040–10041.
24. Shirude,P.S., Gillies,E.R., Ladame,S., Godde,F., Shin-ya,K., Huc,I. and Balasubramanian,S. (2007) Macrocyclic and helical oligoamides as a new class of G-quadruplex ligands. *J. Am. Chem. Soc.*, **129**, 11890–11891.
25. Reed,J.E., Arnal,A.A., Neidle,S. and Vilar,R. (2006) Stabilization of G-quadruplex DNA and inhibition of telomerase activity by square-planar nickel(II) complexes. *J. Am. Chem. Soc.*, **128**, 5992–5993.
26. Jantos,K., Rodriguez,R., Ladame,S., Shirude,P.S. and Balasubramanian,S. (2006) Oxazole-based peptide macrocycles: a new class of G-quadruplex binding ligands. *J. Am. Chem. Soc.*, **128**, 13662–13663.

27. Dixon,I.M., Lopez,F., Tejera,A.M., Esteve,J.-P., Blasco,M.A., Pratviel,G. and Meunier,B. (2007) A G-quadruplex ligand with 10000-fold selectivity over duplex DNA. *J. Am. Chem. Soc.*, **129**, 1502–1503.
28. Green,J.J., Ladame,S., Ying,L., Klenerman,D. and Balasubramanian,S. (2006) Investigating a quadruplex-ligand interaction by unfolding kinetics. *J. Am. Chem. Soc.*, **128**, 9809–9812.
29. Messina,M. and Bennink,M. (1998) Soyfoods, isoflavones and risk of colonic cancer: a review of the in vitro and in vivo data. *Bailliere's Clin. Endocrinol. Metab.*, **12**, 707–728.
30. Hooper,L. and Cassidy,A. (2006) A review of the health care potential of bioactive compounds. *J. Sci. Food Agric.*, **86**, 1805–1813.
31. Kyle,E., Neckers,L., Takimoto,C., Curt,G. and Bergan,R. (1997) Genistein-induced apoptosis of prostate cancer cells is preceded by a specific decrease in focal adhesion kinase activity. *Mol. Pharmacol.*, **51**, 193–200.
32. Polkowski,K. and Mazurek,A.P. (2000) Biological properties of genistein. A review of in vitro and in vivo data. *Acta Pol. Pharm.*, **57**, 135–155.
33. Popiolkiewicz,J., Polkowski,K., Skierski,J.S. and Mazurek,A.P. (2005) In vitro toxicity evaluation in the development of new anticancer drugs-genistein glycosides. *Cancer Lett.*, **229**, 67–75.
34. Lian,F., Li,Y., Bhuiyan,M. and Sarkar,F.H. (1999) p53-independent apoptosis induced by genistein in lung cancer cells. *Nutr. Cancer*, **33**, 125–131.
35. Kato,K., Takahashi,S., Cui,L., Toda,T., Suzuki,S., Futakuchi,M., Sugiura,S. and Shirai,T., (2000) Suppressive effects of dietary genistin and daidzin on rat prostate carcinogenesis. *Jpn. J. Cancer Res.*, **91**, 786–791.
36. Ouchi,H., Ishiguro,H., Ikeda,N., Hori,M., Kubota,Y. and Uemura,H. (2005) Genistein induces cell growth inhibition in prostate cancer through the suppression of telomerase activity. *Int. J. Urol.*, **12**, 73–80.
37. Jagadeesh,S., Kyo,S. and Banerjee,P.P. (2006) Genistein represses telomerase activity via both transcriptional and posttranslational mechanisms in human prostate cancer cells. *Cancer Res.*, **66**, 2107–2115.
38. Guo,J.M., Kang,G.Z., Xiao,B.X., Liu,D.H. and Zhang,S. (2004) Effect of daidzein on cell growth, cell cycle, and telomerase activity of human cervical cancer in vitro. *Int. J. Gynecol. Cancer*, **14**, 882–888.
39. Ravindranath,M.H., Muthugounder,S., Presser,N. and Viswanathan,S. (2004) Anticancer therapeutic potential of soy isoflavone, genistein. *Adv. Exp. Med. Biol.*, **546**, 121–165.
40. Magee,P.J. and Rowland,I.R. (2004) Phyto-oestrogens, their mechanisms of action: current evidence for a role in breast and prostate cancer. *Br. J. Nutr.*, **91**, 513–531.
41. Green,J.J., Ying,L., Klenerman,D. and Balasubramanian,S. (2003) Kinetics of unfolding the human telomeric DNA quadruplex using a PNA trap. *J. Am. Chem. Soc.*, **125**, 3763–3767.
42. Dai,J., Punchihewa,C., Ambrus,A., Chen,D., Jones,R.A. and Yang,D. (2007) Structure of the intramolecular human telomeric G-quadruplex in potassium solution: a novel adenine triple formation. *Nucleic Acids Res.*, **35**, 2440–2450.
43. Agrawal,S., Ojha,R.P. and Maiti,S. (2008) Energetics of the human tel-22 quadruplex-telomestatin interaction: a molecular dynamics study. *J. Phys. Chem. B*, **112**, 6828–6836.
44. Moustakas,D.T., Lang,P.T., Pegg,S., Pettersen,E., Kuntz,I.D., Brooijmans,N. and Rizzo,R.C. (2006) Development and validation of a modular, extensible docking program: DOCK 5. *J. Comput. Aided Mol. Des.*, **20**, 601–619.
45. Ambrus,A., Chen,D., Dai,J., Bialis,T., Jones,R.A. and Yang,D. (2006) Human telomeric sequence forms a hybrid-type intramolecular G-quadruplex structure with mixed parallel/antiparallel strands in potassium solution. *Nucleic Acids Res.*, **34**, 2723–2735.
46. Gaynutdinov,T.I., Neumann,R.D. and Panyutin,I.G. (2008) Structural polymorphism of intramolecular quadruplex of human telomeric DNA: effect of cations, quadruplex-binding drugs and flanking sequences. *Nucleic Acids Res.*, **36**, 4079–4087.
47. Luu,K.N., Phan,A.T., Kuryavyi,V., Lacroix,L. and Patel,D.J. (2006) Structure of the human telomere in K^+ solution: an intramolecular (3 + 1) G-quadruplex scaffold. *J. Am. Chem. Soc.*, **128**, 9963–9970.
48. Phan,A.T., Kuryavyi,V., Luu,K.N. and Patel,D.J. (2007) Structure of two intramolecular G-quadruplexes formed by natural human telomere sequences in K^+ solution. *Nucleic Acids Res.*, **35**, 6517–6525.
49. Miyoshi,D. and Sugimoto,N. (2008) Molecular crowding effects on structure and stability of DNA. *Biochimie*, **90**, 1040–1051.
50. Matsumura,S., Nakano,S.-I. and Sugimoto,N. (2004) Duplex dissociation of telomere DNAs induced by molecular crowding. *J. Am. Chem. Soc.*, **126**, 165–169.
51. Miyoshi,D., Karimata,H. and Sugimoto,N. (2005) Drastic effect of a single base difference between human and tetrahymena telomere sequences on their structures under molecular crowding conditions. *Angew. Chem. Int. Ed.*, **44**, 3740–3744.
52. Xue,Y., Kan,Z.-Y., Wang,Q., Yao,Y., Liu,J., Hao,Y.-H. and Tan,Z. (2007) Human telomeric DNA forms parallel-stranded intramolecular G-quadruplex in K^+ solution under molecular crowding condition. *J. Am. Chem. Soc.*, **129**, 11185–11191.
53. Li,W., Zhang,M., Zhang,J.-L., Li,H.-Q., Zhang,X.-C., Sun,Q. and Qiu,C.-M. (2006) Interactions of daidzin with intramolecular G-quadruplex. *FEBS Lett.*, **580**, 4905–4910.
54. Rosu,F., De Pauw,E., Guittar,L., Alberti,P., Lacroix,L., Mailliet,P., Riou,J.F. and Mergny,J.L. (2003) Selective interaction of ethidium derivatives with quadruplexes: an equilibrium dialysis and electrospray ionization mass spectrometry analysis. *Biochemistry*, **42**, 10361–10371.
55. Larsson,T., Wedborg,M. and Turner,D. (2007) Correction of inner-filter effect in fluorescence excitation-emission matrix spectrometry using Raman scatter. *Anal. Chim. Acta*, **583**, 357–363.
56. Wang,Y. and Patel,D.J. (1993) Solution structure of the human telomeric repeat $d[AG_3(T_2AG_3)_3]$ G-tetraplex. *Structure*, **1**, 263–282.
57. Neidle,S. and Parkinson,G. (2002) Telomere maintenance as a target for anticancer drug discovery. *Nat. Rev. Drug Discov.*, **1**, 383–393.
58. Hurley,L.H. (2002) DNA and its associated processes as targets for cancer therapy. *Nat. Rev. Cancer*, **2**, 188–200.
59. Polkowski,K., Popiołkiewicz,J., Krzeczyński,P., Ramza,J., Pucko,W., Zegrocka-Stendel,O., Boryski,J., Skierski,J.S., Mazurek,A.P. and Grynkiewicz,G. (2004) Cytostatic and cytotoxic activity of synthetic genistein glycosides against human cancer cell lines. *Cancer Lett.*, **203**, 59–69.
60. Yanagihara,K., Ito,A., Toge,T. and Numoto,M. (1993) Antiproliferative effects of isoflavones on human cancer cell lines established from the gastrointestinal tract. *Cancer Res.*, **53**, 5815–5821.
61. Jing,Y. and Waxman,S. (1995) Structural requirements for differentiation-induction and growth-inhibition of mouse erythroleukemia cells by isoflavones. *Anticancer Res.*, **15**, 1147–1152.